The Effect of FEF Microstimulation on the Responses of Neurons in the Lateral Intraparietal Area

Elsie Premereur, Wim Vanduffel, and Peter Janssen

Abstract

■ The macaque FEFs and the lateral intraparietal area (LIP) are high-level cortical areas involved in both spatial attention and oculomotor behavior. Stimulating FEF at a level below the threshold for evoking saccades increases fMRI activity and gamma power in area LIP, but the precise effect exerted by the FEF on LIP neurons is unknown. In our study, we recorded LIP single-unit activity during a visually guided saccade task with a peripherally presented go signal during microstimulation of FEF. We found that FEF microstimulation increased the LIP spike rate immediately after the highly salient go signal inside the LIP receptive field when both target and go signal were presented inside the receptive field, and no other possible go cues were present on the screen. The effect of FEF microstimulation on the LIP response was positive until at least 800 msec after microstimulation had ceased, but reversed for longer trial durations. Therefore, FEF microstimulation can modulate the LIP spike rate only when attention is selectively directed toward the stimulated location. These results provide the first direct evidence for LIP spike rate modulations caused by FEF microstimulation, thus showing that FEF activity can be the source of top–down control of area LIP. ■

INTRODUCTION

To selectively filter the relevant visual signals from the continuous flood of information entering the eye, spatial attention modulates both visual perception and cortical activity (Reynolds & Chelazzi, 2004). The macaque FEFs are thought to be involved in attention-dependent modulations of sensory signals. Indeed, altering activity in FEFs using dopaminergic drugs modulates spike rate activity in area V4 in an attention-like fashion (Noudoost & Moore, 2011). Similarly, electrical microstimulation of the FEF improves contrast detection thresholds (Moore & Fallah, 2001), increases spike rate activity in V4 (Moore & Armstrong, 2003), enhances gamma power in the lateral intraparietal area (LIP; Premereur, Vanduffel, Roelfsema, & Janssen, 2012), and modulates fMRI activity in early visual cortex in an attention-like manner (Premereur, Janssen, & Vanduffel, 2013; Ekstrom, Roelfsema, Arsenault, Bonmassar, & Vanduffel, 2008).

In addition to its role in spatial attention, FEF is part of a parietofrontal network involved in saccade planning, including LIP (Wardak, Olivier, & Duhamel, 2011; Koyama et al., 2004; Nobre, Gitelman, Dias, & Mesulam, 2000; Corbetta et al., 1998). LIP neurons are strongly modulated by spatial attention and saccadic eye movements (Bisley & Goldberg, 2010; Colby & Goldberg, 1999; Snyder, Batista, & Andersen, 1997), and inactivation of area LIP causes deficits in visual search tasks (Wardak, Olivier, & Duhamel, 2004). Furthermore, anatomical studies have shown reciprocal connections between areas FEF and LIP (Anderson, Kennedy, & Martin, 2011; Schall, Morel, King, & Bullier, 1995; Stanton, Bruce, & Goldberg, 1995). Previous research has shown that stimulation of area FEF not only evokes antidromic activity in area LIP but can also orthodromically activate LIP neurons (Ferraina, Paré, & Wurtz, 2002). The latter study, however, did not investigate the functional significance of FEF-induced spike rate increases in LIP. Hence, it is unclear whether enhanced responses of LIP neurons at attended locations represent the source of endogeneous attentional control (Gottlieb, 2002) or if it arises from the influence of top–down signals originating in frontal areas such as the FEF (Ibos, Duhamel, & Ben Hamed, 2013).

To examine the effect FEF neurons could have on LIP, we recorded the responses of single LIP neurons to the brightening of a go cue inside the neuron's receptive field (RF) in a visually guided saccade (VGS) task while stimulating the FEF with currents below the threshold for evoking saccades. We found that FEF stimulation caused a highly selective increase in the LIP response to the go cue brightening when both the target and go cue were positioned inside the LIP RF. The effect was present only when the FEF saccade vector was aligned with the LIP RF, and when no additional stimuli were presented outside the LIP RF. Our study provides the first direct evidence that the macaque FEF can influence the responses of LIP neurons to salient events occurring inside the RF.

KU Leuven

Journal of Cognitive Neuroscience 26:8, pp. 1672–1684
doi:10.1162/jocn_a_00591

METHODS

Subjects and Surgery

All experiments were performed using two juvenile male rhesus monkeys (monkeys K and T: 4 kg). After training to sit in a primate chair, a custom-made headpost was implanted on the skull using ceramic screws and dental acrylic. At least 6 weeks after surgery, the monkeys began training in eye movement tasks.

Details of the surgical procedures have been described elsewhere (Premereur et al., 2013; Premereur, Vanduffel, Roelfsema, et al., 2012; Ekstrom et al., 2008). Briefly, after 2–4 months of training, 43 platinum–iridium wire electrodes (Teflon-coated microwire, 25 μm diameter, 90% platinum, 10% iridium) were chronically implanted in area FEF in the left hemisphere, along the rostral bank of the arcuate sulcus, at a depth of 3–5 mm. Approximately 40 μm of Teflon was stripped from the wire tips before insertion. Three electrodes were implanted between skin and muscle to serve as ground. Electrodes were connected with a MRI-compatible connector (Omnetics, Minneapolis, MN) and typically had impedances in the range of 5–200 kΩ.

Three to four weeks after electrode implantation, a craniotomy was made, and an MRI-compatible recording cylinder (Crist Instruments, Hagerstown, MD) was implanted parallel to the intraparietal sulcus. All surgeries were performed under isoflurane (1–2%) anesthesia and sterile conditions. Cylinders were implanted over the left hemisphere (Horsley–Clark coordinates 10-11P and 14-18L; Figure 1A). To verify the recording positions, we inserted glass capillaries filled with a 2% copper sulfate solution into the recording grid (Crist Instruments) at several grid positions and acquired structural MR images (0.6 mm resolution; Figure 1A). All procedures were performed in accordance with the National Institute of Health's Guide for the Care and Use of Laboratory Animals and were approved by the ethical committee of the KU Leuven Medical School.

Stimuli and Tests

All stimuli were displayed on a Philips Brilliance 202P4 CRT monitor operating at 120 Hz at a viewing distance of 86 cm.

VGS Tasks

Monkeys had to maintain fixation within a window (max size = 2° × 2°) around a small red spot in the center of the display for a fixed duration of 450 msec, after which a single green saccade target and a gray go cue appeared (single-cue VGS task; Figure 1B). Target and go cue were equal in size (0.25°) and luminance (6 cd/m^2). Both target and go cue could appear either inside the LIP RF or at the opposite position ipsilateral to the recording cylinder, thus creating four different conditions: target and go

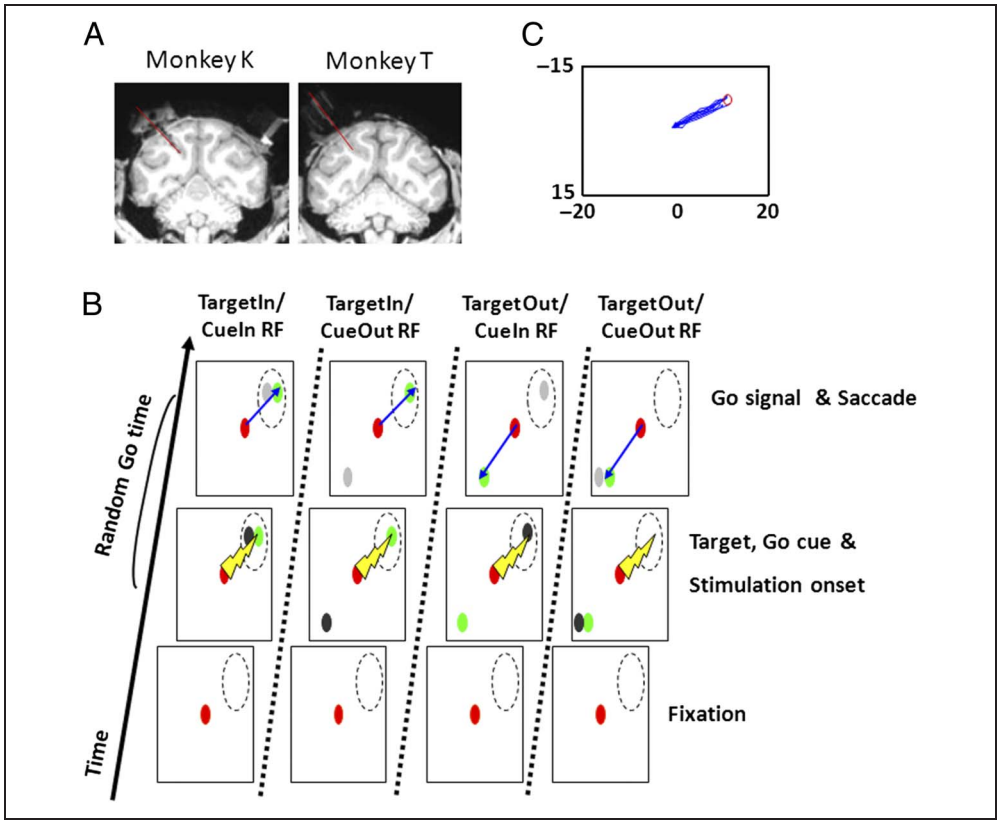

Figure 1. Methods. (A) T1-weighted anatomical MRIs of monkeys K and T. Red lines show representative recording positions. (B) Single-cue VGS task. After a brief period of fixation, a gray go cue and a green saccade target appeared on the screen. Both stimuli could be positioned inside or outside the RF (dotted circle) in interleaved trials. In half of the trials, FEF-EM started together with target and go cue onset, and the movement vector pointed toward the RF. After a variable delay, the go cue changed its luminance, indicating to the monkey to saccade toward the green target (represented by the blue arrow). (C) Example saccade vector. Blue paths represent eye traces during FEF stimulation. Red circle shows the median endpoint of the eye traces.

cue in RF, target in RF and go cue out, go cue in RF and target out, and both target and go cue out of RF. After a variable delay (between 500 and 2000 msec), the luminance of the go cue was increased by 300%. This increase in luminance was the go signal indicating to the animal when to make a saccade toward the green target. Henceforth, we will refer to the go cue as the gray dot appearing either inside or outside the LIP RF and to the go signal as the brightening of this go cue. The animal had to saccade toward the target within 500 msec after the go signal and hold fixation in a 3°–4° window surrounding the target for 250 msec, after which he obtained the reward. To encourage fast responses, reward size was governed by an exponential function of RT between 150 and 500 msec after the go signal. The time between target onset and the go signal was a random value drawn from a unimodal Weibull distribution delayed by 500 msec (Janssen & Shadlen, 2005),

$$U(t) = \begin{cases} 3\alpha\left(t-\frac{1}{2}\right)^2 e^{-\alpha\left(t-\frac{1}{2}\right)^3} & \text{for } t > 1/2 \\ 0 & \text{Otherwise} \end{cases} \quad (1)$$

The median go time for all correct trials was 1077 msec with 10% of the go times longer than 1350 msec.

In addition to this VGS task (single-cue VGS task), a saccade task with multiple possible go cues was used (multiple-cue VGS task), using the same stimulus, timing, and reward parameters. The same distribution of go times $U(t)$ (1) was used in both saccade tasks. In this version of the saccade task, four possible gray go cues and one green saccade target were used (Premereur, Vanduffel, Roelfsema, et al., 2012). The saccade target appeared either inside the LIP RF (multipleCue–TargetIn condition) or at the opposite position, ipsilateral with respect to the recording cylinder (multipleCue–TargetOut condition). The possible go cues appeared in the upper and lower quadrants ipsilateral and contralateral to the RF, with one of them always appearing inside the RF. After a variable delay (between 500 and 2000 msec), the luminance of one of the possible go cues (selected at random) was increased by 300%, indicating to the animal to saccade toward the green target. Thus, in multipleCue–TargetIn trials, a saccade target and a possible go cue (which could become the go signal in 25% of the trials) appeared inside the LIP RF, whereas in multipleCue–TargetOut trials, only a possible go cue appeared inside the RF.

Recording Procedure

The position of the right eye was recorded at a sampling rate of 500 Hz using an EyeLink 1000 eye tracker (SR Research, Ontario, Canada). A photocell attached to the monitor detected the onset of a white square in the lower right corner of the screen (covered with black tape to obscure it from the monkeys' view) that appeared in the first video frame containing a stimulus (target onset or go signal). Tungsten microelectrodes (impedance at 1 kHz: 0.8–1.2 MΩ, FHC, Bowdoinham, ME) were inserted by means of a hydraulic microdrive (FHC) through a stainless steel guide tube positioned in a plastic grid (spacing 1 mm, Crist Instruments). Spiking activity was amplified and filtered to 300–5000 Hz. Eye position signals, neural activity, and photocell pulses were digitized and processed at 20 kHz on a digital signal processor (C6000 series; Texas Instruments, Dallas, TX). Spikes were discriminated on-line with the digital signal processor using a dual time window discriminator and were displayed using LabView (National Instruments, Austin, TX) and custom-designed software.

In a typical recording session, the electrode was lowered into the lateral bank of the intraparietal sulcus while the monkey made delayed VGSs. We searched for responses in single-unit activity by placing saccade targets at various locations in the contralateral hemifield. Formal testing started once a spatially selective single-unit target response was observed. Significant delay period activity during memory-guided saccades was also observed in these electrode penetrations (Premereur, Vanduffel, & Janssen, 2011). Importantly, the only criterion for inclusion was that the neuron demonstrated spatially selective saccadic activity, as described in previous studies of visual salience in LIP (Premereur, Vanduffel, & Janssen, 2012; Premereur et al., 2011; Falkner, Krishna, & Goldberg, 2010).

Microstimulation

FEF microstimulation (FEF-EM) started simultaneously with target and go cue onset and lasted for 500 msec. Because the distribution of go times for the saccade tasks was unimodal between 500 and 2000 msec after target onset, EM always ceased before even the shortest go time (524 msec) occurred. The electrical and visual stimulation events were controlled by custom-designed software (LabView, National Instruments, Austin, TX).

At the beginning of every recording session, 5–10 FEF electrodes were tested to determine the saccade vector and the minimum voltage necessary for evoking saccades. Monkeys performed a passive fixation task while voltage was applied by means of an eight-channel digital stimulator (DS8000, WPI, Houston, TX). Stimulation trains for evoking saccades lasted for 200 msec (pulse width: 0.48 msec, 100 Hz) and consisted of biphasic square-wave pulses. The saccade threshold was determined as the minimum current necessary for generating a saccade: Typically, this was the current that evoked saccades in at least 60% of 6–12 trials (between 12 and 110 μA; mean threshold = 59.5 μA, *SEM* = 3.1 μA). Note that the thresholds described in this experiment are slightly higher than typically described in FEF stimulation (FEF-EM) experiments (<50 μA; Bruce, Goldberg, Bushnell, & Stanton, 1985), most likely because of the chronic implantation, which can induce growth of a fibrous barrier between the

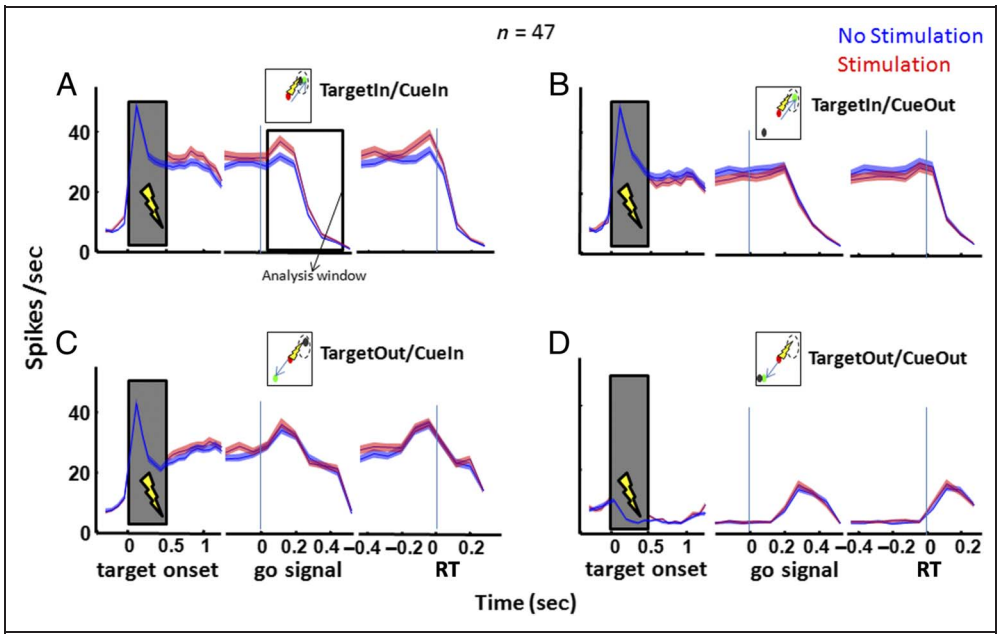

Figure 2. Spike rate data during the VGS task. (A) Average spike rate for the TargetIn/CueIn condition, for all neurons tested with the FEF movement vector aligned to the LIP RF. Spike rates in the left are aligned on target onset, in the middle on go signal, and in the right on RT. No-stimulation trials are shown in blue, stimulation trials in red. Shaded areas represent standard errors. Graphics in each figure show the stimulus configuration on the screen (RF shown with dotted circles). Spike rates were not analyzed in the 500-msec stimulation interval (marked with the gray box). (B) TargetIn/CueOut condition. (C) TargetOut/CueIn condition. (D) TargetOut/CueOut condition.

electrodes and neural tissue (Ekstrom et al., 2008) and because of the blunt tips of the electrodes (Tehovnik, 1996). The endpoint of the saccade vector was calculated as the median endpoint of eye traces obtained during suprathreshold FEF stimulation (typically 4–8 evoked saccades; see Figure 1C).

After finding a target-selective neuron in area LIP, an FEF electrode was chosen with its movement field (MF) aligned with the LIP RF, and the saccade target and go cue were positioned at the endpoint of the saccade vector (and at the opposite location; see Figure 1B). Although we did not systematically map the RFs of the LIP neurons, the strong responses to target onset indicated that the calculated position of the saccade target was indeed inside the LIP RF (see Figure 2A and B, leftmost panels; aligned on target onset).

During recording, the pulse width was either maintained at 0.48 msec or reduced to 0.16 msec (biphasic square wave pulse: 0.24 msec pos, 0.24 neg or 0.08 msec pos, 0.08 msec neg) to reduce stimulation artifacts in the recording signal (Premereur, Vanduffel, Roelfsma, et al., 2012); stimulation intensity was always set to one third of the saccade threshold. We have previously shown that suprathreshold stimulation of FEF at 100 Hz and 0.16 msec pulse width evoked saccades in the majority of the FEF sites (Premereur, Vanduffel, Roelfsma, et al., 2012), with saccade metrics similar to those obtained when stimulating with a 0.48 msec pulse width.

Data Analysis

All data analysis (unless stated otherwise) was performed using custom-written Matlab (The Mathworks, Natick, MA) programs.

The average spike rate aligned on target onset and plotted in 80 msec bins included all spikes up to 50 msec after the go signal to ensure that the data contained no effects from the go signal or saccade execution. Because the go times varied between 500 and 2000 msec, plots in which the spikes were aligned on the go signal or on RT contained data from trials ending at different times after stimulation offset. All spikes that fell within the stimulation interval (0–500 msec) were excluded from the analysis to avoid possible artifacts from the electrical stimulation. For each recording site, the spatial selectivity of the response was tested using paired t tests ($p < .05$) comparing mean spike rate after target onset (0–200 msec) to baseline activity (200 msec before target onset).

To test the effect of FEF-EM, permutation tests were performed. This nonparametric statistical test was chosen to compare mean values in nonnormally distributed data (Kolmogorov–Smirnov statistic = 0.9005, $p < .001$). For the permutation test, spike rate data from both stimulation and no-stimulation trials were grouped together in a large vector. This vector was then randomly shuffled 10,000 times, and for every permutation, the difference between the first n_1 trials (with n_1 = number of no-stimulation trials) and the last n_2 trials (with n_2 = number of stimulation trials) was calculated. p values were calculated by the percentage of permuted differences exceeding the real difference in spike rate between stimulation and no-stimulation trials. For population analyses, trials of all neurons were pooled as in a previous study (Premereur et al., 2011). As we typically only have one to two trials per neuron with a go signal shorter than 800 msec (i.e., the interval immediately following the end of the microstimulation epoch), all trials were pooled to obtain the most reliable estimate for these short trials. To rule out the possibility that a large sample size (675 trials for the

TargetIn/CueIn–NoStimulation condition, 702 trials for the TargetIn/CueIn–Stimulation condition) artificially increased significance, all results were verified in various subpopulations of neurons (e.g., each monkey individually; different neuronal response types). To exclude the possibility that trials with an exceedingly low or high spike rate influenced our results, all results were verified by calculating for every trial the normalized rate (divide every trial by the average spike rate per neuron in the 500–700 msec interval after target onset in the TargetIn/CueIn condition).

We did not analyze spikes occurring during the stimulation interval, as the stimulation artifact was too large to detect spikes reliably. Therefore, similar to Moore and Armstrong (2003), we investigated only the time period following the stimulation interval.

To investigate the relationship between the effect of electrical FEF-EM on the LIP spike rates and the offset of EM, we analyzed LIP responses to the go signal as a function of the interval between stimulation offset and go signal onset. For single neurons, we grouped the trials according to their go time in 200 msec bins (sliding window analysis with 10 msec increments), aligned the spikes on the time of the go signal for each trial and calculated the firing rate in the interval (80–480 msec) after the go signal for EM and no-EM trials. The difference in spike rate between EM and no-EM trials was then plotted as a function of the time interval between EM offset and go signal onset. We performed linear regression analysis to determine the slope and the intercept of the linear fit to the data. For group data (all trials pooled together), the same analysis was performed but on nonoverlapping 100 msec windows.

RT was defined as the point in time when the velocity of the eye trace exceeded five times the standard deviation of the velocity in the interval from 700 until 100 msec before the go signal (typically in the range of 120–170°/sec; see Premereur et al., 2011).

For all latency analyses, spike rate data were binned using a 20-msec window. The exact onset time of the stimulation-induced increase in spike rate was defined as the center of the first of two consecutive 20 msec bins with a significant difference between EM and no-EM trials (permutation test, $p < .01$). The timing of presaccadic enhancement and go signal response was determined as the center of the first of two consecutive 20 msec with a significant spike rate increase compared with two bins back, permutation test, $p < .01$).

To capture the diversity of the neural population with respect to anticipatory climbing activity, the spike rate data were fitted with a weighted sum of two functions: the subjective hazard rate associated with a unimodal distribution of go times and an exponential distribution with a mean of 0.2 (Premereur et al., 2011).

$$R(t) = w_c + w_{uni}A_{uni}(t-\tau) + w_{exp}E(t) + \varepsilon \qquad (2)$$

where R is the neuronal response, w_c is a constant term, and w_{uni} and w_{exp} are the weights for the unimodal anticipation function and the exponential function, respectively, with A_{uni} delayed by time shift τ, which was fixed at -0.1 sec. ε represents noise, which is assumed to be Gaussian with uncertainty derived from the sample means. We used a maximum-likelihood fitting procedure to obtain the fits, parameter estimates, and their standard errors. A positive weight for the subjective hazard and negative weight for the exponential distribution indicated anticipatory climbing activity (anticipatory neurons), whereas nonanticipatory neurons (visual neurons) were characterized by a negative weight for the subjective hazard and a positive weight for the exponential.

RESULTS

We recorded single-cell activity in spatially selective LIP neurons while the animals performed a VGS task (Figure 1B). As in our previous studies (Premereur, Vanduffel, & Janssen, 2012; Premereur et al., 2011), LIP neurons were not selected based on memory delay period activity: The only criterion for inclusion was spatially selective saccadic activity. However, these neurons were generally located in proximity (<1000 μm) to neurons displaying memory delay period activity (Premereur et al., 2011). During the saccade task, FEF was randomly stimulated in half of the trials at one third of the saccade threshold (i.e., between 6 and 55 μA). Data were collected in 31 neurons in monkey K and 54 neurons in monkey T. In 47 of these 85 neurons (monkey K: 15, monkey T: 32), the FEF-EM vector was directed toward the LIP RF.

Effect of FEF-EM on the LIP Response to the Go Signal

In our single-cue VGS task, only one go cue and one target were used, both of which could be placed inside or outside the LIP RF, thus creating four conditions (Figure 1B). Because the stimulation artifact could not be removed from the recording traces, we focused on the effect of FEF-EM on the LIP response to the go signal, which always occurred after the EM interval.

In the TargetIn/CueIn condition, FEF-EM (with the saccade vector directed toward the LIP RF) evoked a significant increase in LIP spike rates shortly after the go signal (permutation test 80–480 msec after go signal, $p = .004$; spike rate rises from 16.6 to 19.4 spikes/sec, an increase of 17% above the mean; Figure 2A, middle, black outline). Note that a similar significant increase in the LIP firing rate was obtained when calculating significance in the 0–480 msec interval after the go signal ($p = .0064$). This increase was present in both animals individually (permutation test: monkey K: $p < .001$; monkey T: $p = .03$). Furthermore, the effect was verified using a parametric t test (t stat: -2.72; $df = 1375$; $p = .007$) and a

nonparametric Wilcoxon rank sum test ($p = .056$) and in normalized spike rate (permutation test: $p = .02$). No effect of FEF-EM on the LIP activity after the go signal was found in any of the other three conditions (Figure 2B–D, permutation tests, 80–480 msec after go signal: $p > .16$ for all three conditions). Thus, FEF-EM induced a specific and significant increase in LIP spike rate after the go signal when both the saccade target and the go signal (TargetIn/CueIn) appeared inside the LIP RF, but not when either the go signal (TargetOut/CueIn) or target (TargetIn/CueOut) were positioned alone inside the RF, nor when both target and go signal were positioned outside the LIP RF (TargetOut/CueOut). It is important to emphasize that the effect of FEF-EM on LIP activity shown in Figure 2 represents an average of trials ending at different moments in time (ranging from 40 to 1500 msec) after EM had ceased. (The time dependency of the FEF-EM effect on LIP will be discussed below.) A two-way ANOVA (factors: Stimulation × Target/CuePosition) however, showed, no significant main effect of EM ($F = 1.48$, $df = 1$, $p = .22$) nor a significant interaction ($F = 1.57$, $df = 3$, $p = .2$; but see below for a time-dependent effect). Note that the increase in spike rate that we measured in LIP cannot be a microstimulation artifact because it was specific for one condition and because only those spikes were included that were detected after the offset of EM.

In the plot of LIP activity aligned on RT (Figure 2A–D, right), it is evident that the effect of FEF-EM was largely confined to the interval preceding the time of the saccade (see Figure 2A, rightmost panel; the increase in EM-evoked spike rate started 170 msec before RT with a 2.6 spikes/sec EM-induced increase in the 160–80 msec interval before RT (permutation test: $p = .01$) and a 5.4 spikes/sec increase in the 80–0 msec interval before RT (permutation test: $p = .008$). Because the RT in the TargetIn/CueIn condition averaged 205.32 ± 2.00 msec (monkey K) and 188.12 ± 2.10 msec (monkey T), FEF-EM could have increased the LIP response to the go signal or, alternatively, increased the presaccadic enhancement that is present for saccades directed toward the RF. The TargetIn/CueOut (Figure 2B) and the TargetOut/CueIn (Figure 2C) conditions, however, could distinguish between these two possibilities. The activity before RT in the TargetIn/CueOut condition (Figure 2B) represents presaccadic enhancement (Colby, Duhamel, & Goldberg, 1996; go cue brightened outside the RF and the saccade was directed toward the RF) starting 40 msec before the RT and thus much later than the EM-induced increase in spike rate (170 msec before RT). The activity in the TargetOut/CueIn condition (Figure 2C), however, represents a response to the brightening of the go cue inside the RF, which started at 140 msec before the RT. Therefore, the temporal dynamics of the FEF-EM effect on LIP activity in the TargetIn/CueIn condition, starting 170 msec before RT, were clearly more similar to those of the go signal response, starting 140 msec before RT, rather than those of the presaccadic enhancement, which started only 40 msec before RT (compare the middle panel of Figure 2A to that in Figure 2C). Note also that the late response in the TargetOut/CueOut condition represents a postsaccadic response elicited by saccades directed outside the LIP RF. Thus, FEF-EM primarily induces stronger visual responses to salient events in the RF of LIP neurons when such events are aligned with an eye movement.

FEF-EM did not affect the average RT in any of the conditions (permutation test, $p > .05$ for all four conditions; the time dependency of the effect of FEF-EM on RT will be discussed below) or the animals' performance (number of correct trials for no-EM TargetIn/CueIn trials: 14.36, standard error of the mean (SEM): 0.90; average number of correct trials for EM trials: 14.94, SEM: 0.84; average number of incorrect trials for no-EM TargetIn/CueIn trials 23.27, SEM: 1.71; average number of incorrect trials for EM TargetIn/CueIn trials: 23.67, SEM: 1.86).

FEF-EM also tended to induce a smaller increase in LIP spike rates in the time interval after the EM epoch and before the go signal, in trials where the go cue appeared inside the LIP RF, that is, TargetIn/CueIn and TargetOut/CueIn trials (activity aligned on target onset in Figure 2A and C, left): the average spike rate in the −200 to 0 msec interval before the go signal was slightly higher in EM trials than in no-EM trials (although not significant: $p = .1$ for TargetIn/CueIn and TargetOut/CueIn separately; $p = .03$ for both conditions combined). This small increase in spike rate before the go signal supports the interpretation that the EM-induced increase in spike rate is unrelated to presaccadic enhancement. No significant FEF-EM effect was present when the go cue appeared outside the RF (Figure 2B and D, middle). Thus, FEF-EM elicited a small increase in LIP spike rate when the go cue appeared inside the LIP RF and an elevated LIP response to the brightening of the go cue (i.e., the go signal) in the LIP RF when both target and go cue appeared inside the RF.

We obtained significant EM-induced increases in LIP activity immediately after the go signal in 8/47 single neurons (two-tailed permutation test, 80–480 msec after go signal, $p < .05$; see Figure 3). Note that one neuron showed a significant decrease in spike rate. It should be pointed out that the EM-induced increase in average LIP spike rate was not caused by these significant neurons alone as this effect remained even when the significant neurons were excluded from the analysis (permutation test, $p = .02$). In comparing the RTs for trials obtained during the recording of these eight neurons, we found that FEF-EM increased the animals' RTs (no-EM: 195.7; EM: 205.5; permutation test: $p < .05$), and this increase was mainly present for the shortest trials (i.e., trials in which the go signal occurred shortly after EM offset: linear fit of RT data plotted versus go signal time; intercept no-EM: 237.4 ± 41.8; EM: 285.6 ± 33.1, an effect that was not present throughout the entire population of neurons [$p < .05$] nor in the 39 nonsignificant neurons

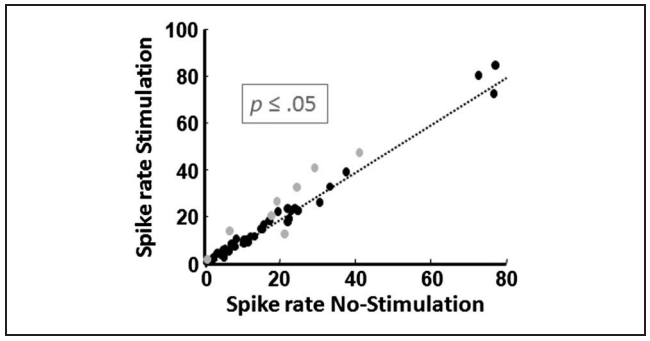

Figure 3. Single neurons. For every neuron, the average spike rate in the 80–480 msec interval after the go signal was calculated for the TargetIn/CueIn condition. Gray dots show neurons with a significant stimulation-induced spike rate modulation.

[$p < .05$]). On the assumption that FEF-EM modulates the spike rate of several neurons throughout LIP, the significant effect of FEF-EM on RT in neurons that were significantly modulated suggests that the EM parameters were most optimal for these neurons, for example, because of better alignment of MF and RF or because of more appropriate current levels.

To investigate the influence of the EM parameters on the LIP response we varied the width of the EM pulse. In the majority of the recording sessions presented above ($n = 32/47$) we stimulated FEF at one third of the saccade threshold with a 0.48 msec pulse width, whereas a pulse width of 0.16 msec was used in the remainder of the sessions ($n = 15/47$). For the neurons of both data sets, we found a significant EM-induced increase in LIP spike rate shortly after the go signal (pulse width, 0.48 msec: $n = 32, p = .04$; pulse width, 0.16 msec: $n = 15, p = .02$). The latter finding is consistent with our previous experiment (Premereur, Vanduffel, Roelfsma, et al., 2012), which showed that varying the pulse width for FEF-EM does not affect the saccade metrics.

Spatial and Task Specificity of FEF-EM-induced LIP Responses

To test the spatial specificity of the FEF-EM effect on LIP activity, we also recorded activity from LIP neurons whose RF was not aligned with the FEF saccade vector ($n = 38$). In these control neurons, the saccade vector and the LIP RF were located in different quadrants of the contralateral hemifield (i.e., in the case where the LIP RF was positioned in the upper left quadrant, an FEF electrode with a MF in the lower left quadrant was chosen; see Figure 4A, inset) or were separated by at least 15°. No significant EM-induced increase was found in these control cells in the TargetIn/CueIn condition (permutation test on spike rate activity 80–480 msec following go signal, $p = .13$; Figure 4A), nor in any of the other three conditions ($p > .12$). These results demonstrate that the FEF-EM-induced effect on LIP neurons was spatially specific.

Furthermore, we stimulated FEF during a VGS task with four possible go cues ($n = 35$, multiple-cue VGS task; see Premereur, Vanduffel, Roelfsema, et al., 2012) and again found no effect for FEF-EM around the time of the go signal, neither in the condition in which both target and go signal (i.e., the dimming of the go cue; see pictogram in Figure 4B) were positioned inside the RF (Figure 4B, permutation test, $p = .45$) nor in any of the other conditions ($p > .15$ for all conditions). Similarly, FEF-EM did not affect RTs in the multiple-cue VGS tasks (permutation test, $p > .05$ corrected for multiple comparisons for

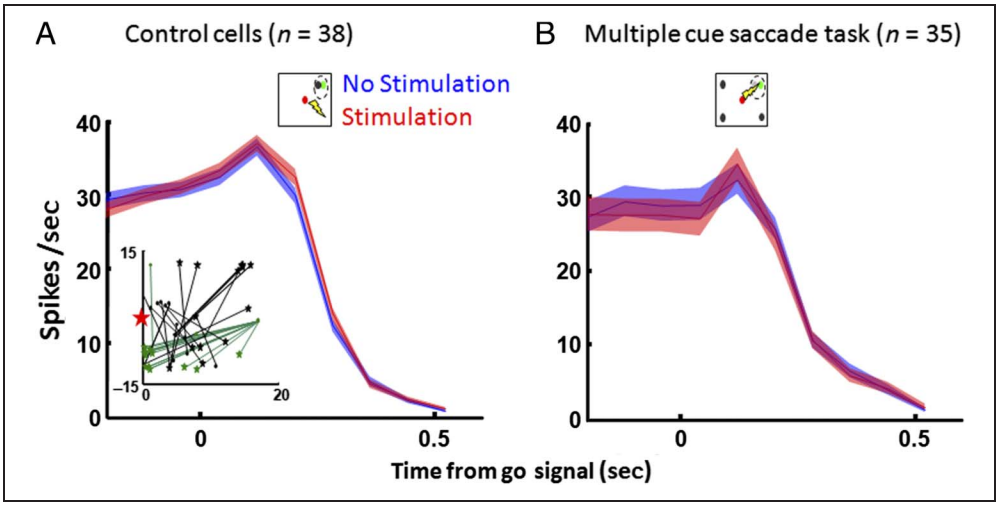

Figure 4. Control experiments. (A) Average spike rate during the VGS task. Spike rates are shown for the TargetIn/CueIn condition, with the stimulation vector pointing away from the RF. Spikes are aligned on go signal. Figure properties as in Figure 2. Graphic shows stimulus configuration. Inset shows RF and MF positions for monkeys T (black) and K (green). Lines connect RF position (marked with circle) to MF positions (stars) for every recording session. (B) Average spike rate during the VGS task with multiple possible go cues. FEF movement vector is directed toward the RF. Spike rates are shown for the condition where the possible go cue appearing inside the RF becomes the go signal.

all conditions; see also Premereur, Vanduffel, Roelfsema, et al., 2012). Even in the subset of neurons for which both the single-cue and the multiple-cue VGS tasks were tested ($n = 11$), we found a significant EM-induced increase in LIP spike rate following the go signal in the single-cue VGS task ($p = .03$) in the TargetIn/CueIn condition, but not in the multiple-cue VGS task in the TargetIn/CueIn condition ($p = .17$). Note that we previously obtained significant increases in LFP power in LIP during the multiple-cue saccade task (Premereur, Vanduffel, Roelfsema, et al., 2012). However, LFPs were not measured for the LIP neurons presented here.

Thus far, we have found that FEF-EM elicits an increase in LIP spike rate immediately after the go signal but before the eye movement, although only in the condition with both the go signal and saccade target inside the RF. Furthermore, the effect of FEF-EM on LIP spike rate is absent when possible go cues appear outside the RF; this effect is spatially specific, in that it exists only when the saccade vector and the LIP RF are aligned; moreover, it is obtained using either wide or narrow EM pulses.

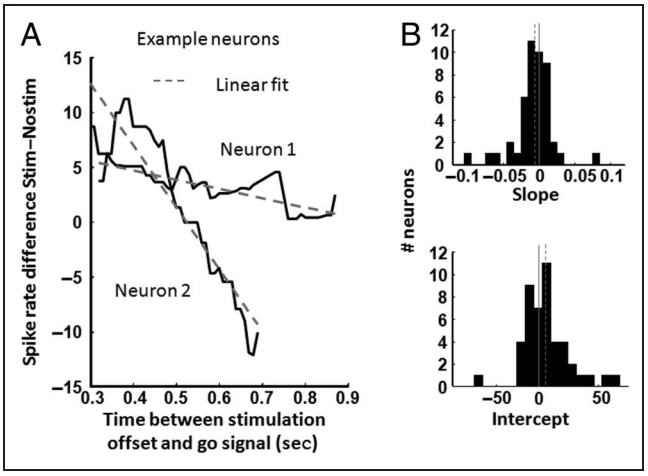

Figure 5. Time dependency, single neurons. (A) Example neurons. For every go time (represented as the difference between stimulation offset and go signal), the increase in spike rate (stimulation–no-stimulation) in the 80–480 msec interval following the go signal was calculated using a sliding window analysis (200 msec window, step size 10 msec). Data were fitted using linear regression analysis (dashed lines). (B) Distribution of slopes and intercepts obtained in the linear fit for single neurons. Dashed lines represent median; full line indicates zero.

Time Dependency of the FEF-EM Effect on LIP Responses and on RT

In the saccade tasks, the go times (i.e., the time between target onset and the go signal) were drawn from a unimodal distribution ranging from 500 to 2000 msec (median go time = 1077 msec), but FEF-EM always started at target onset and lasted for 500 msec. Because trials ended at different time points after FEF-EM had ceased, we investigated whether the effect of FEF-EM depended on the time between EM offset and the time of the go signal. Indeed, in comparing the average spike rate for short trials (go time < 1000), we found a significant interaction between EM and Target/Go Cue Position (two-way ANOVA: $F = 2.48$; $df = 1$; $p = .05$), which was not present for long trials (go time > 1000 msec: $F = 1.06$; $df = 3$; $p = .36$) or for all trials combined ($F = 1.57$; $df = 3$; $p = .2$, see above). We therefore grouped all TargetIn/CueIn trials according to their go time to plot the increase in spike rate (200 msec sliding window; step size = 10 msec) within the interval (80–480 msec) after the go signal in EM trials compared with no-EM. In both single-cell examples shown in Figure 5A, the spike rate was elevated in the first epoch after FEF-EM offset (linear fit: intercept 12.27 and 58.03 for neuron 1 and neuron 2, respectively, $p < .05$). However, the effect of FEF-EM was reduced (example neuron 1) or even reversed (example neuron 2) in trials where the go signal appeared more than ~500–800 msec after the end of FEF-EM (slope = −0.008 and −0.06 for Neuron 1 and Neuron 2, respectively, $p < .05$). Note that the two plots do not start and stop at the same time since the time of the go signal was a random variable and not every time bin contained sufficient trials. To investigate the time dependency of the FEF-EM effect on the LIP population, we performed a similar analysis for all neurons ($n = 46$, one neuron was excluded because of insufficient number of trials).

We obtained a median slope of −0.0051 (Wilcoxon test; $p < .05$) and a median intercept of 8.03 (Wilcoxon test: $p = .01$; median $R^2 = .41$; Figure 5B). Of the individual neurons with an $R^2 > .4$ (i.e., that half of the neuronal population with the best fit), 16 neurons were found with a significantly negative slope and a significantly positive intercept, indicating that the effect of EM is largest shortly after the end of EM and slowly degrades over time (note that eight neurons with an $R^2 > .40$ showed a significantly positive slope, and throughout the entire population, 23 neurons were found with a significantly negative slope). The latter analysis suggests that the small effect on individual neurons (only 7/47 neurons with a significant EM-induced increase in spike rate following the go signal) was most likely because of the time dependency of the FEF-EM effect and an insufficient number of short trials (go time < 800 msec) in individual neurons.

Figure 6 shows the average spike rates for all trials of all 47 neurons in no-EM and EM trials as a function of the time elapsing between the end of EM and the go signal (100 msec window) for the four conditions in the single-cue VGS task. For trials of the TargetIn/CueIn condition (Figure 6A) in which the time between EM offset and the go signal was less than 850 msec, the LIP spike rate following the go signal was higher in FEF-EM trials than in no-EM trials, an effect that was greatest in the shortest trials: FEF-EM increased the average LIP spike rate by

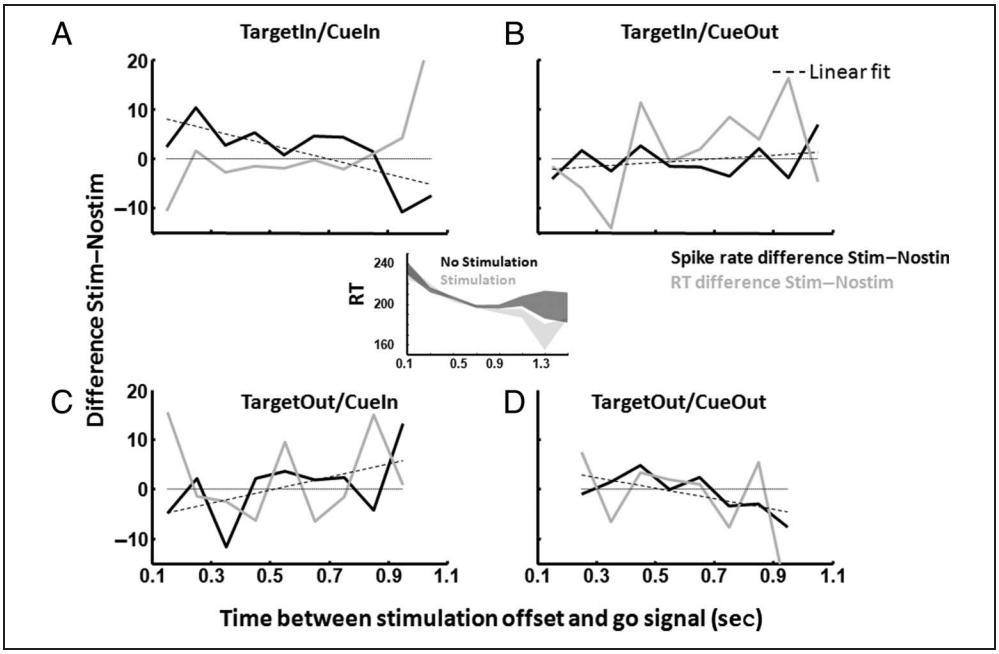

Figure 6. Time dependency, population analysis. Black curves show the increase in spike rate (stimulation–no-stimulation) in the 80–480 msec interval following the go signal. Trials were grouped according to their go times, and spike rates in the 80–480 msec interval following go signal were calculated using a sliding window analysis (100 msec window). Data were fitted using linear regression analysis (marked with the dashed lines). Gray curves show a similar analysis for the RT difference. The center inset shows the average RT for stimulation and no-stimulation trials averaged over all four conditions.

as much as 55% of the firing rate in trials ending within 250 msec after EM offset and by 30% when the go signal came as late as 600–800 msec after EM offset. Remarkably, for even longer trials (go signal > 920 msec after the end of FEF-EM), the average LIP spike rate after the go signal was lower in FEF-EM trials than in no-EM trials, averaging 32% less than the mean LIP spike rate. A linear fit to the data yielded a slope of −0.015, which was significantly less than zero (95% CI [−0.03, −0.003]) and an intercept of 17.5 (95% CI [4.3, 30.7]). Hence, the FEF-EM-induced increase in the LIP response around the go signal, as illustrated in Figure 2A (which did not take the go time into account), represents an average of (a majority of) trials with enhanced responses and (a minority of) trials with response suppression. Note that data were plotted only if more than 20 trials occurred with a go time within the interval, thereby excluding the shortest and longest trials: Because the go times were randomly drawn from a unimodal distribution, only 4% of the trials had go times between 500 and 700 msec and 11% of the trials had go times longer than 1350 msec (i.e., 850 msec after EM offset). The results were confirmed by applying the linear fit on the average spike rate difference over time calculated per cell (200 msec sliding window, 10 msec stepwidth: intercept: 6.94; slope = −0.005; $p < .05$).

Figure 6B–D shows that, in the other conditions of the single-cue VGS task, FEF-EM exerted no effect on the LIP spike rate: TargetIn/CueOut: slope = 0.0039, 95% CI [−0.0052, 0.013]; TargetOut/CueIn: slope = 0.014, 95% CI [−0.006, 0.033]; TargetOut/CueOut: slope = −0.011, 95% CI [−0.022, 0.001].

For comparison, the same analysis was performed on the trials obtained during the multiple-cue VGS task (TargetIn/CueIn condition) and for the control cells in which the FEF saccade vector was not aligned with the LIP RF. In both experiments, the differences in spike rate were centered around zero, and we found no significant EM-induced increase in spike rate for any of the go times (control neurons: slope = 0.0031; $p > .05$; multiple-cue VGS: slope = −0.004; $p > .05$). Thus, FEF-EM caused an increase in LIP spike rates after the go signal, and this increase was greater in trials ending shortly after EM offset. The FEF-EM effect even reversed for longer trials (>920 msec after EM had ceased).

The inset in Figure 6 shows the average RT across conditions in EM and no-EM trials. As in previous studies (Premereur et al., 2011; Janssen & Shadlen, 2005), the average RT decreased sharply for longer go times, mirroring the rising conditional probability that the go signal would occur given that it had not yet appeared (the hazard function). Although FEF-EM did not affect RT in the majority of trials, the average RT was significantly longer in EM trials compared with no-EM trials when the go signal came more than 1270 msec after target onset (0.77 sec after EM offset). Indeed, we obtained a main effect of EM for trials with a go time longer than 1270 msec (two-way ANOVA with factors EM [Stim–NoStim] and condition [TargetIn/CueIn, TargetIn/CueOut, TargetOut/CueIn, TargetOut/CueOut]; $F_{\text{Stimulation}} = 4.54$, $df = 1$, $p = .03$; $F_{\text{condition}} = 6.93$, $df = 3$, $p = .0001$; $F_{\text{interaction}} = 0.55$, $df = 3$, $p = .65$). Thus, FEF-EM significantly slows down RTs, but only for the longest trials.

We also plotted the average difference in RTs between EM and no-EM trials as a function of go time for each of the four conditions separately in Figure 6A–D (gray traces). We obtained a significant increase in RT (permutation test, $p = .04$) for the longest trials (go times >

1400 msec) in the TargetIn/CueIn condition when FEF-EM was applied (Figure 5A). The interval during which the RTs were longer after FEF-EM (>1400 msec) coincided remarkably well with the interval in which we observed a decrease in the LIP response to the go signal caused by FEF-EM (see Figure 5A, time between EM offset and go signal 900–1000 msec, which equals 1400–1500 msec after target onset). However, RTs also tended to be longer in the longest EM trials in the TargetIn/CueOut (trials > 1400 msec; Figure 5B, gray trace; permutation test: p = .14) and TargetOut/CueIn (Figure 5C, p = .22), which were conditions without significant decreases in the LIP spike rate (Figure 5B–C). Moreover for the longest EM trials in the TargetIn/CueIn condition, the spike rate after the go signal did not correlate with RT (r = −0.06; p = .12). Therefore, our data do not permit to conclude that the lower LIP response to the go signal caused by FEF-EM is associated with a longer RT.

Although previous research suggested a greater effect of EM immediately after EM offset (Moore & Fallah, 2004), we did not find a significant influence of EM on RT in even the shortest trials (go time < 800 msec; thus trials ending no later than 300 msec after EM offset), neither for all trials combined (permutation test; p = .32), nor for only the trials in the TargetIn/CueIn condition (p = .59) or other conditions (p > .19). Importantly, however, because of the unimodal distribution of our go times, only 9% of trials (i.e., 453, EM and no-EM trials combined, or only 60 trials in the TargetIn/CueIn-NoEM conditions and only 72 trials in the TargetIn/CueIn-EM condition) were shorter than 800 msec.

Anticipatory versus Visual Neurons

We have previously described LIP neurons as either anticipatory, that is, showing climbing activity in the delay period before the saccade, or nonanticipatory with stronger responses to salient events such as the brightening of the go cue in the RF (Premereur et al., 2011). This same classification scheme was applied to our neuronal population to determine if the EM-induced increase in spike rate differed between the two types of neurons. Although there was a small but nonsignificant increase in spike rate in anticipatory neurons (n = 19; permutation test: p = .144; Figure 7B), the effect of FEF-EM was much more pronounced in nonanticipatory, visual LIP neurons (n = 28; p = .0053; Figure 7A), and most (6/8) neurons with a significant effect of FEF-EM were visual. However, a significant interaction effect was not observed (ANOVA, [No-EM–EM × anticipatory–nonanticipatory], F = 1.02, df = 1, p = .313). Note that both types of neurons also did not show an EM-induced increase in spike rate in any of the other conditions (permutation test, p > .05).

Finally, we performed the time dependency analysis on the TargetIn/CueIn trials recorded in visual and anticipatory neurons separately (Figure 7C–D) and found that the slope was significantly smaller than 0 for the visual neurons, but not for the anticipatory neurons (visual neurons: slope = −0.02; p < .05; anticipatory neurons: slope = −0.008; p > .05). Furthermore, the intercept was significantly positive only for visual neurons (visual neurons: 27.83; p < .05; anticipatory neurons: intercept: 11; p > .05) Thus, both the magnitude and the time dependency

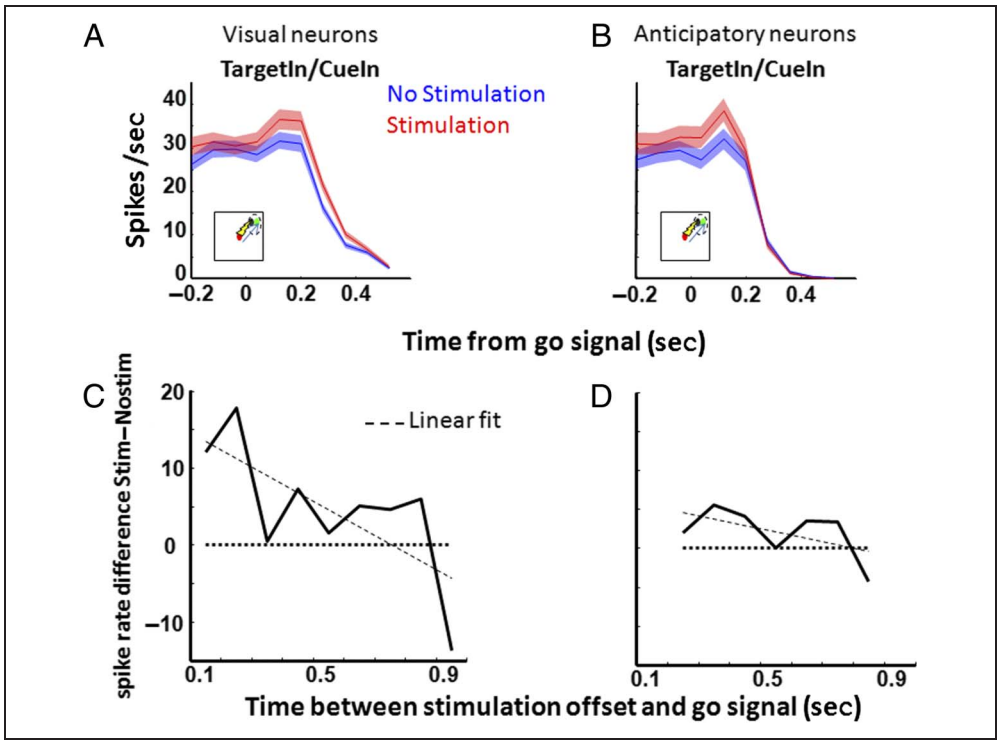

Figure 7. (A, B) Average spike rate aligned on go signal for visual (A) and anticipatory (B) neurons in the TargetIn/CueIn condition. (C, D) Black curves show the increase in spike rate (stimulation–no-stimulation) in the 80–480 msec interval following the go signal. Trials were grouped according to their go times, and spike rates in the 80–480 msec interval following go signal were calculated using a sliding window analysis (100 msec windows). Data were fitted using linear regression analysis (marked with the dashed lines).

of the FEF-EM effect on LIP neurons were larger in visual compared with anticipatory neurons.

DISCUSSION

Our study provides the first direct evidence that the macaque FEF can influence the responses of single LIP neurons to salient events occurring in their RFs. We observed a highly selective increase in the LIP response to the go signal after FEF-EM, but only when a saccade was planned toward the LIP RF. Furthermore, the effect was only present when the FEF saccade vector was aligned with the LIP RF, and no other stimuli were presented outside the LIP RF.

Electrically stimulating FEF influences spike activity in V4 (Moore & Armstrong, 2003) and fMRI activity in area LIP and throughout the visual cortex (Premereur et al., 2013; Ekstrom et al., 2008). In both studies, the stimulation-induced effects in visual cortex were strongest in the presence of distractors. Here, we have shown that the stimulation-induced increase in LIP spike rate following the go signal disappeared in the presence of multiple possible go cues outside the RF or when the target and go cue appeared at different locations in the visual field (TargetOut/CueIn condition). Previous studies have demonstrated that the saccade target automatically attracts attention (Bisley & Goldberg, 2003; Kowler, Anderson, Dosher, & Blaser, 1995). Therefore, the animals in our study had to actively divide their attention to detect the go signal as soon as possible, whereas the distractors in the study by Ekstrom et al. (2008) and Moore and Armstrong (2003) could be ignored. Thus, our results suggest that the effect of FEF-EM on LIP can be observed under conditions of selective spatial attention (toward the LIP RF), but not during divided attention.

Ibos et al. (2013) compared responses in FEF and LIP neurons during an attention–orientation target detection task, in which monkeys were cued to attend to one hemifield to detect a target embedded in a stream of distractors. On the basis of the analysis of the neuronal latencies and the proportions of cue- and target-selective neurons in FEF and LIP, the authors hypothesized that enhancement of the LIP response to behaviorally relevant stimuli may be the result of top–down influences originating in the FEF. Our study provides the first causal evidence that the FEF can indeed modulate LIP responses to salient events occurring in the RFs of LIP neurons during selective attention. The activity in LIP can be viewed as a priority map of the environment (Bisley & Goldberg, 2010), which can transiently shift toward the location of a distractor flashed in the visual field (Bisley & Goldberg, 2003) or toward the location of the go cue when it brightens (Premereur et al., 2011). Therefore, our results also imply that FEF-EM can influence the activity in LIP, at least when attention is directed to a single location in the visual field.

Although our results show that FEF can modulate the LIP response to salient events, our study does not imply that all saliency or attention-related responses in area LIP are the result of top–down influences from area FEF. In fact, the latency of target detection by LIP neurons (~50 msec; Premereur et al., 2011), precludes a significant contribution from FEF during the earliest phase of bottom–up visual processing in LIP.

Functional interactions between FEF and LIP have been demonstrated previously (Miller & Buschman, 2013). Synchronized activity has been observed between these two areas during pop-out (gamma band) and visual search (beta band; Buschman & Miller, 2007). Moreover, reversible inactivation studies have demonstrated the interdependency of FEF and area LIP (Chafee & Goldman-Rakic, 2000), and previous monkey fMRI studies have reported strong LIP activations following FEF-EM (Ekstrom et al., 2008) during passive fixation and a VGS task (Premereur et al., 2013). Our study characterizes the precise effect exerted by FEF-EM on LIP: FEF-EM induces a spatially specific increased saliency response in LIP.

Area LIP is a functionally heterogeneous area (Meister, Hennig, & Huk, 2013), with a subpopulation of LIP neurons showing anticipatory activity before the saccade mimicking the subjective hazard rate (Premereur et al., 2011). Many LIP neurons, however, do not show an increased spike rate over time. Not surprisingly, we found that the FEF stimulation-induced increase in the LIP response to the go signal was most pronounced within this dominant population (60% in the current study) of nonanticipatory, visual neurons, which are also more influenced by salient visual events (Premereur et al., 2011).

Stimulating FEF at a level below the level that is required for evoking saccades can enhance behavioral performance (Gerits et al., 2012; Moore & Fallah, 2001). However, the exact timing of the FEF-EM relative to the monkey's response greatly influences the behavioral effect (Moore & Fallah, 2004). The lack of any behavioral effect in our study is most likely because of the timing of the stimulation, which was not related to the timing of the go signal. Similarly, in the current single-cue experiment, FEF-EM did not affect the LIP response to the go signal when the target appeared outside the LIP RF (TargetOut/CueIn condition). Increased competition between stimuli in the visual field, which is known to enhance inhibitory interactions between LIP neurons (Falkner et al., 2010), may have obscured the effect of FEF-EM on LIP in those conditions. We previously showed that in the multiple-cue VGS task and during microstimulation, FEF-EM causes a spatially specific and task-specific increase in low gamma power in the LFP in LIP (Premereur, Vanduffel, Roelfsema, et al., 2012) for saccades directed toward the RF. We did not record LFPs in this experiment, but given the close relationship between spikes and high gamma power (Premereur, Vanduffel, & Janssen 2012; Ray & Maunsell, 2011; Liu & Newsome, 2006), it is likely

that FEF-EM also induced stronger gamma oscillations in LIP following the go signal in the single-cue task of this study.

The timing of the FEF-EM effect on LIP is also relevant for its interpretation. As expected, the strongest modulation (up to 50% of the mean firing rate) was measured in the first epoch (100–300 msec) after FEF-EM had ceased. Surprisingly, FEF-EM continued to exert an excitatory influence on the LIP response to the go signal up to 700–900 msec after the end of microstimulation. Beyond this interval, the LIP response was unexpectedly lower in stimulation trials compared with no-stimulation trials. Thus, the FEF-EM effect was similar to a priming effect on the LIP response to the go signal within approximately 800 msec after the end of microstimulation, an interval within which most trials ended. For the small minority of trials (11%) that ended more than 850 msec after EM had ceased (i.e., more than 1350 msec after target onset), the effect of FEF-EM on LIP was negative, although the probability that the go signal would appear given that it had not yet occurred (i.e., the hazard rate) was very high in this time interval. Therefore, the FEF-EM effect on LIP did not follow the hazard function (high when the hazard was low and vice versa).

Several factors may explain why we did not observe shorter RTs after FEF-EM in the majority of trials (those ending <850 msec after the end of microstimulation). First, the brightening of the go cue was always suprathreshold (a luminance increase of 300%), whereas the effects of both spatial attention and FEF-EM are known to be strongest when low-contrast stimuli are used (Ekstrom, Roelfsema, Arsenault, Kolster, & Vanduffel, 2009; Reynolds, Pasternak, & Desimone, 2000). Furthermore, both animals were highly overtrained in the task (RTs as low as 180 msec for the longest trials), so that the effect of FEF-EM may have been obscured by a ceiling effect. Finally, our FEF-EM epoch was fixed to the first 500 msec after target onset, which was unrelated to the timing of the go signal (Moore & Fallah, 2004). The only behavioral effect we observed was an increase in RT after FEF-EM when restricting the analysis to the LIP cells that were significantly affected by FEF-EM, which may be related to better alignment of the LIP RF and the FEF movement vector or to more optimal stimulation parameters. Similarly, a previous study observed increases in RT caused by FEF-EM (Burman & Bruce, 1997).

Both LIP and FEF have been implicated in the allocation of spatial attention (Wardak, Ibos, Duhamel, & Olivier, 2006; Wardak et al., 2004; Moore & Armstrong, 2003; Nobre et al., 2000; Corbetta et al., 1998). FEF-EM enhances the responses of neurons in the visual cortex in a spatially specific manner when stimuli appear inside the FEF MF (Moore & Armstrong, 2003), and LIP neurons are more active when an animal covertly directs its attention to the LIP RF (Goldberg, Colby, & Duhamel, 1990). Could the FEF-EM effect on LIP indicate that FEF is a source of attention-related (or saliency-related) response modulations in LIP? In other words, does FEF modulate the LIP responses to salient events occurring at attended locations? A more direct demonstration that attention-related modulation of the LIP response is evoked by FEF input would require LIP recordings and precisely targeted FEF inactivations, which would by themselves cause deficits in any visual search task (Wardak et al., 2006). Nevertheless, our data provide direct and causal evidence consistent with Ibos et al. (2013), implicating FEF as a source of input that enhances the visual responses of LIP neurons to behaviorally relevant events.

Reprint requests should be sent to Peter Janssen, Neuro-en Psychofysiologie, KU Leuven, Herestraat 49, Bus 1021, Leuven, Belgium, 3000, or via e-mail: peter.janssen@med.kuleuven.be.

REFERENCES

Anderson, J. C., Kennedy, H., & Martin, K. A. (2011). Pathways of attention: Synaptic relationships of frontal eye field to V4, lateral intraparietal cortex, and area 46 in macaque monkey. *Journal of Neuroscience, 31,* 10872–10881.

Bisley, J. W., & Goldberg, M. E. (2003). Neuronal activity in the lateral intraparietal area and spatial attention. *Science, 299,* 81–86.

Bisley, J. W., & Goldberg, M. E. (2010). Attention, intention, and priority in the parietal lobe. *Annual Review of Neuroscience, 33,* 1–21.

Bruce, C. J., Goldberg, M. E., Bushnell, M. C., & Stanton, G. B. (1985). Primate frontal eye fields. II. Physiological and anatomical correlates of electrically evoked eye movements. *Journal of Neurophysiology, 54,* 714–734.

Burman, D. D., & Bruce, C. J. (1997). Suppression of task-related saccades by electrical stimulation in the primate's frontal eye field. *Journal of Neurophysiology, 77,* 2252–2267.

Buschman, T. J., & Miller, E. K. (2007). Top–down versus bottom–up control of attention in the prefrontal and posterior parietal cortices. *Science, 315,* 1860–1862.

Chafee, M. V., & Goldman-Rakic, P. S. (2000). Inactivation of parietal and prefrontal cortex reveals interdependence of neural activity during memory-guided saccades. *Journal of Neurophysiology, 83,* 1550–1566.

Colby, C. L., Duhamel, J. R., & Goldberg, M. E. (1996). Visual, presaccadic, and cognitive activation of single neurons in monkey lateral intraparietal area. *Journal of Neurophysiology, 76,* 2841–2852.

Colby, C. L., & Goldberg, M. E. (1999). Space and attention in parietal cortex. *Annual Review of Neuroscience, 22,* 319–349.

Corbetta, M., Akbudak, E., Conturo, T. E., Snyder, A. Z., Ollinger, J. M., Drury, H. A., et al. (1998). A common network of functional areas for attention and eye movements. *Neuron, 21,* 761–773.

Ekstrom, L. B., Roelfsema, P. R., Arsenault, J. T., Bonmassar, G., & Vanduffel, W. (2008). Bottom–up dependent gating of frontal signals in early visual cortex. *Science, 321,* 414–417.

Ekstrom, L. B., Roelfsema, P. R., Arsenault, J. T., Kolster, H., & Vanduffel, W. (2009). Modulation of the contrast response function by electrical microstimulation of the macaque frontal eye field. *Journal of Neuroscience, 29,* 10683–10694.

Falkner, A. L., Krishna, B. S., & Goldberg, M. E. (2010). Surround suppression sharpens the priority map in the lateral intraparietal area. *Journal of Neuroscience, 30,* 12787–12797.

Ferraina, S., Paré, M., & Wurtz, R. H. (2002). Comparison of cortico-cortical and cortico-collicular signals for the generation of saccadic eye movements. *Journal of Neurophysiology, 87,* 845–858.
Gerits, A., Farivar, R., Rosen, B. R., Wald, L. L., Boyden, E. S., & Vanduffel, W. (2012). Optogenetically induced behavioral and functional network changes in primates. *Current Biology, 22,* 1722–1726.
Goldberg, M. E., Colby, C. L., & Duhamel, J. R. (1990). Representation of visuomotor space in the parietal lobe of the monkey. *Cold Spring Harbor Symposia on Quantitative Biology, 55,* 729–739.
Gottlieb, J. (2002). Parietal mechanisms of target representation. *Current Opinion in Neurobiology, 12,* 134–140.
Ibos, G., Duhamel, J. R., & Ben Hamed, S. (2013). A functional hierarchy within the parietofrontal network in stimulus selection and attention control. *Journal of Neuroscience, 33,* 8359–8369.
Janssen, P., & Shadlen, M. N. (2005). A representation of the hazard rate of elapsed time in macaque area LIP. *Nature Neuroscience, 8,* 234–241.
Kowler, E., Anderson, E., Dosher, B., & Blaser, E. (1995). The role of attention in the programming of saccades. *Vision Research, 35,* 1897–1916.
Koyama, M., Hasegawa, I., Osada, T., Adachi, Y., Nakahara, K., & Miyashita, Y. (2004). Functional magnetic resonance imaging of macaque monkeys performing visually guided saccade tasks: Comparison of cortical eye fields with humans. *Neuron, 41,* 795–807.
Liu, J., & Newsome, W. T. (2006). Local field potential in cortical area MT: Stimulus tuning and behavioral correlations. *Journal of Neuroscience, 26,* 7779–7790.
Meister, M. L., Hennig, J. A., & Huk, A. C. (2013). Signal multiplexing and single-neuron computations in lateral intraparietal area during decision-making. *Journal of Neuroscience, 33,* 2254–2267.
Miller, E. K., & Buschman, T. J. (2013). Cortical circuits for the control of attention. *Current Opinion in Neurobiology, 23,* 216–222.
Moore, T., & Armstrong, K. M. (2003). Selective gating of visual signals by microstimulation of frontal cortex. *Nature, 421,* 370–373.
Moore, T., & Fallah, M. (2001). Control of eye movements and spatial attention. *Proceedings of the National Academy of Sciences, U.S.A., 98,* 1273–1276.
Moore, T., & Fallah, M. (2004). Microstimulation of the frontal eye field and its effects on covert spatial attention. *Journal of Neurophysiology, 91,* 152–162.
Nobre, A. C., Gitelman, D. R., Dias, E. C., & Mesulam, M. M. (2000). Covert visual spatial orienting and saccades: Overlapping neural systems. *Neuroimage, 11,* 210–216.
Noudoost, B., & Moore, T. (2011). Control of visual cortical signals by prefrontal dopamine. *Nature, 474,* 372–375.
Premereur, E., Janssen, P., & Vanduffel, W. (2013). FEF microstimulation causes task-dependent modulation of occipital fMRI activity. *Neuroimage, 67,* 42–50.
Premereur, E., Vanduffel, W., & Janssen, P. (2011). Functional heterogeneity of macaque lateral intraparietal neurons. *Journal of Neuroscience, 31,* 12307–12317.
Premereur, E., Vanduffel, W., & Janssen, P. (2012). Local field potential activity associated with temporal expectations in the macaque lateral intraparietal area. *Journal of Cognitive Neuroscience, 24,* 1314–1330.
Premereur, E., Vanduffel, W., Roelfsema, P. R., & Janssen, P. (2012). Frontal eye field microstimulation induces task-dependent gamma oscillations in the lateral intraparietal area. *Journal of Neurophysiology, 108,* 1392–1402.
Ray, S., & Maunsell, J. H. (2011). Different origins of gamma rhythm and high-gamma activity in macaque visual cortex. *PLoS Biology, 9,* e1000610.
Reynolds, J. H., & Chelazzi, L. (2004). Attentional modulation of visual processing. *Annual Review of Neuroscience, 27,* 611–647.
Reynolds, J. H., Pasternak, T., & Desimone, R. (2000). Attention increases sensitivity of V4 neurons. *Neuron, 26,* 703–714.
Schall, J. D., Morel, A., King, D. J., & Bullier, J. (1995). Topography of visual cortex connections with frontal eye field in macaque: Convergence and segregation of processing streams. *Journal of Neuroscience, 15,* 4464–4487.
Snyder, L. H., Batista, A. P., & Andersen, R. A. (1997). Coding of intention in the posterior parietal cortex. *Nature, 386,* 167–170.
Stanton, G. B., Bruce, C. J., & Goldberg, M. E. (1995). Topography of projections to posterior cortical areas from the macaque frontal eye fields. *Journal of Comparative Neurology, 353,* 291–305.
Tehovnik, E. J. (1996). Electrical stimulation of neural tissue to evoke behavioral responses. *Journal of Neuroscience Methods, 65,* 1–17.
Wardak, C., Ibos, G., Duhamel, J. R., & Olivier, E. (2006). Contribution of the monkey frontal eye field to covert visual attention. *Journal of Neuroscience, 26,* 4228–4235.
Wardak, C., Olivier, E., & Duhamel, J. R. (2004). A deficit in covert attention after parietal cortex inactivation in the monkey. *Neuron, 42,* 501–508.
Wardak, C., Olivier, E., & Duhamel, J. R. (2011). The relationship between spatial attention and saccades in the frontoparietal network of the monkey. *European Journal of Neuroscience, 33,* 1973–1981.